

Received December 30, 2019, accepted January 12, 2020, date of publication January 17, 2020, date of current version January 27, 2020.

Digital Object Identifier 10.1109/ACCESS.2020.2967413

Wideband Wearable Antenna for Biomedical Telemetry Applications

AMOR SMIDA^{1,2}, AMJAD IQBAL^{3,4}, (Student Member, IEEE), ABDULLAH J. ALAZEMI⁵, (Member, IEEE), MOHAMED I WALY^{6,7}, RIDHA GHAYOULA^{8,9}, AND SUNGHWAN KIM¹⁰

¹Department of Medical Equipment Technology, College of Applied Medical Sciences, Majmaah University, AlMajmaah 11952, Saudi Arabia

²Unit of Research in High Frequency Electronic Circuits and Systems, Faculty of Mathematical, Physical, and Natural Sciences of Tunis, Tunis El Manar University, Tunis 2092, Tunisia

³Centre For Wireless Technology, Faculty of Engineering, Multimedia University, Cyberjaya 63100, Malaysia

⁴Department of Electrical Engineering, CECOS University of IT and Emerging Sciences, Peshawar 25000, Pakistan

⁵Department of Electrical Engineering, Faculty of Engineering and Petroleum, Kuwait University, Kuwait 13060, Kuwait

⁶Department of Medical Equipment Technology, College of Applied Medical Sciences, Majmaah University, AlMajmaah 11952, Saudi Arabia

⁷Department of Biomedical Engineering and System, Higher Institute of Engineering, El Shorouk Academy, Al Shorouk 11837, Egypt

⁸Department of Electrical and Computer Engineering, Laval University, Quebec, QC G1V0A6, Canada

⁹Unit of Research in High Frequency Electronic Circuits and Systems, Faculty of Mathematical, Physical and Natural Sciences of Tunis, Tunis El Manar University, Tunis 2092, Tunisia

¹⁰School of Electrical Engineering, University of Ulsan, Ulsan 44610, South Korea

Corresponding authors: Amjad Iqbal (aiqbal@ieee.org) and Sunghwan Kim (sungkim@ulsan.ac.kr)

This work was supported in part by the Research Program through the National Research Foundation of Korea under Grant NRF-2019R1A2C1005920 and in part by the Deanship of Scientific Research at Majmaah University for funding this work under Project 1439-86.

ABSTRACT This paper presents a wideband, low-profile and semi-flexible antenna for wearable biomedical telemetry applications. The antenna is designed on a semi-flexible material of RT/duroid 5880 ($\epsilon_r = 2.2$, $\tan\delta = 0.0004$) with an overall dimensions of 17 mm \times 25 mm \times 0.787 mm ($0.2\lambda_o \times 0.29\lambda_o \times 0.009\lambda_o$). A conventional rectangular patch is modified by adding rectangular slots to lower the resonant frequency, and the partial ground plane is modified to enhance the operational bandwidth. The final antenna model operates at 2.4 GHz with a 10-dB bandwidth (fractional bandwidth) of 1380 MHz (59.7 % at the centre frequency of 2.4 GHz). The proposed antenna maintains high gain (2.50 dBi at 2.4 GHz) and efficiency (93 % at 2.4 GHz). It is proved from the simulations and experimental results that the antenna has negligible effects in terms of reflection coefficient, bandwidth, gain, and efficiency when it is bent. Moreover, the antenna is simulated and experimentally tested in proximity of the human body, which shows good performance. The proposed wideband antenna is a promising candidate for compact wearable biomedical devices.

INDEX TERMS On-body antenna, wideband antenna, wearable antenna, SAR, flexible antenna, biomedical antenna.

I. INTRODUCTION

In recent ages, a significant interest is developed towards the flexible/semi-flexible devices to be worn for biomedical telemetry applications. Using flexible/semi-flexible materials is gaining a lot of attention for developing wearable nodes [1]. Advances in wearable technology are seen with the development of implantable devices for healthcare applications such as; endoscopy [2], [3], neural recording [4], glucose monitoring [5], and intracranial pressure monitoring [6], [7].

The associate editor coordinating the review of this manuscript and approving it for publication was Wanchen Yang^{1b}.

The wearable antenna is a key component of the wearable network as it is responsible for receiving and transmitting the signal between the implantable device and wearable network [8], [9]. The antenna should be made as efficient as possible because the human body is a lossy platform for EM waves and a lot of EM waves are absorbed by the body as heat and energy [10]. A special design consideration is required for the antenna to have minimum backward radiations (Specific Absorption Rate (SAR)) which results in damaging the human tissues [11]. At the same time, special care is required for the overall size of the antenna [12]. The overall size of the antenna need to be as small as possible.

Several types of wearable antennas have been developed in the past. The authors of [13] designed a fractal antenna for 2.4 GHz applications. The fractional bandwidth of the antenna is only 7.75 % and a small detuning because of the human body loading may lead to impedance mismatch at the desired frequency band. Also, the antenna is not suitable to be integrated with a compact wearable receiver. The authors of [14] designed a compact ($0.065\lambda_0 \times 0.065\lambda_0$) triangular patch antenna, however, the antenna has very narrow operating bandwidth. A low-sized cpw-fed slot antenna with floating ground plane for ISM band is designed in [15], however, the designed antenna possesses very low fractional bandwidth (6 % at the center frequency of 5.825 GHz). Several other wearable antennas such as electromagnetic bandgap (EBG) based antennas [16], [17], and substrate integrated waveguide (SIW) based antennas [18]–[20] were designed, however, all these antennas have a narrow bandwidth. In [21], a wearable antenna using a fabric material as a substrate, knitted copper as patch, and ground plane is designed for medical applications, however, the overall dimensions of the antenna are large to be used in any compact environment. In [22], a flexible antenna operating at 2.4 GHz, with a circular polarization is designed for body-worn applications. The antenna's circular polarization is achieved by designing edge-cuts and side slit in the radiating patch. A thicker polyimide spacer is used as a substrate while nickel-plated textile is used as a radiating element and ground plane. In [23], different miniaturization techniques are used to design a low profile wearable button antenna for WLAN applications with an omni-directional radiation pattern, using a flexible Velcro material as a substrate. In [24], a UHF RFID tag antenna using flexible textile material is designed with the help of T-matching stub. The size of the antenna is large to limit its applications in a compact system-in-package (SIP) applications. In [25], a wearable antenna (circular patch and rectangular ground plane) for ISM band is designed using indigo jeans as a substrate. In [26], a CPW fed graphene and carbon nanotube-based flexible antenna is designed for ISM band by utilizing a flexible substrate of poly-dimethylsiloxane. It is always challenging to reduce the size of wearable antenna and maintain the antenna performance at good range. Several attempts have been made to reduce size of the wearable antenna such as shorting pins [27], quarter mode designs [20], using high permittivity materials [28], increasing the current path by increasing the resonator length [29], and reactive loading [30], etc. The antenna size is reduced significantly using the mentioned techniques, however, new challenges emerge such as low efficiency, complex designs, and narrow bandwidths. Also, the modern communication system architecture demands ultra-compact components along with a simple design. Designing antenna with such characteristics is always a challenging task to accomplish. On the other side, waves absorbed by the human tissue is another problem in the wearable antennas. The portion of power absorbed by the human tissue is described through a parameter known as specific absorption rate (SAR). Different

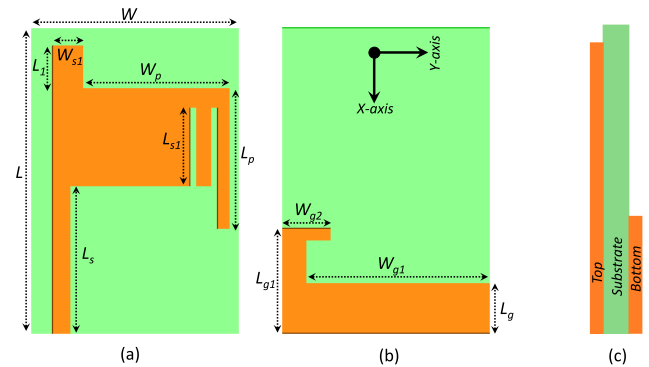


FIGURE 1. Proposed wearable antenna: (a) top view [$W = 17$, $L = 25$, $L_s = 12.1$, $L_1 = 3.5$, $W_{s1} = 2.5$, $W_p = 12$, $L_p = 11.5$, $L_{s1} = 6.4$ (unit = mm)], (b) bottom view [$W_{g1} = 15$, $W_{g2} = 4$, $L_{g1} = 4.1$, $L_{g2} = 8.6$ (unit = mm)], and (c) side view.

methods have been adopted in antenna design for lowering the SAR rate [17], [18], [31]–[36]. In [31], a ferrite sheet is utilized between the antenna and human body for reducing the SAR value. Use of a ferrite sheet reduces backward radiation as well as has less impact on rest of the antenna parameters. In [32], SAR is reduced as well as efficiency is enhanced by placing a PEC between the antenna and human body. In [17], [18], [33]–[35], a metamaterial structure is designed between the antenna and human body to lower the SAR value. Utilizing metamaterial structures in the antenna minimizes the SAR, while efficiency and gain of the antenna increase significantly.

In this paper a low-profile and wideband wearable antenna is designed for 2.4 GHz band. Main advantages of the designed antenna are as follows:

- To the best of our knowledge, this is the compact antenna for an ISM band (2.4 GHz) with a wide 10-dB operational and fractional bandwidth.
- The proposed antenna has acceptable performance in terms of operating bandwidth, gain and efficiency in the bending scenarios.
- Also, the antenna has favorable gain, acceptable bandwidth and high efficiency in on-body worn scenarios. Moreover, the antenna has reasonable low SAR value when mounted on the human body.

II. ANTENNA DESIGN

Fig. 1a, 1b, and 1c portray the top, bottom and side view of the proposed wearable antenna, respectively. A semi-flexible material of RT/duroid 5880 ($\epsilon_r = 2.2$, $\tan\delta = 0.0004$) having the thickness of 0.787 mm is used as a substrate. The radiating element is excited with a 50Ω transmission line backed by a partial ground plane. The overall dimensions of the antenna are $17\text{ mm} \times 25\text{ mm} \times 0.787\text{ mm}$ ($0.2\lambda_0 \times 0.29\lambda_0 \times 0.009\lambda_0$). The initial dimensions of the radiator were calculated using standard equations for microstrip patch [37]. The proposed antenna is basically a modified form of the conventional rectangular patch antenna. Modifying the

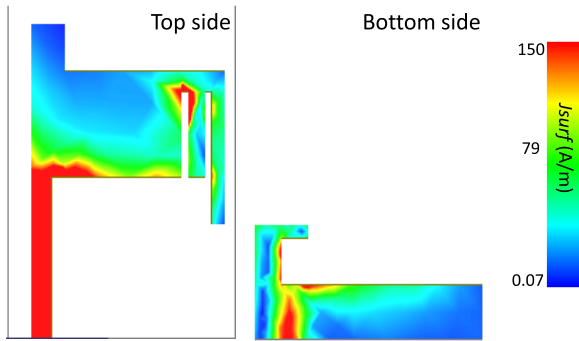


FIGURE 2. Surface current distribution of the antenna at 2.4 GHz.

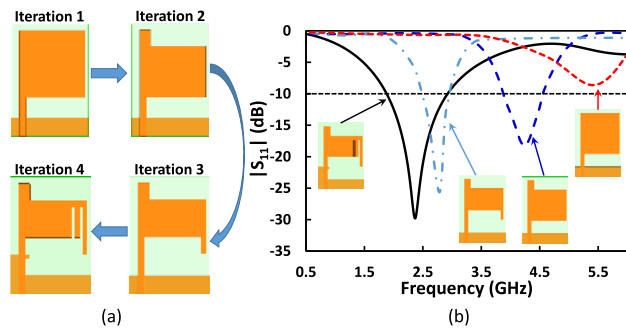


FIGURE 3. (a) Design evolution steps, and (b) corresponding reflection coefficient ($|S_{11}|$) of the wearable antenna.

ground plane and etching slots in the main radiator reduces the overall size of the antenna as well as assess in impedance matching at the desired band. The surface current density (J_{surf}) of the antenna at 2.4 GHz is portrayed in Fig. 2.

A. DESIGN EVOLUTION

The design evolution steps and their corresponding reflection coefficient ($|S_{11}|$) graph is illustrated in Fig. 3a and 3b, respectively. The design process started with a simple truncated ground plane rectangular patch antenna. In that iteration (Iteration 1), the antenna had one resonance at around 5.5 GHz, but the antenna was not matched at the resonance frequency. The antenna in iteration 1 was modified in iteration 2. A rectangular portion from the upper part of the patch was etched in order to get impedance matching and to achieve miniaturization [38]. In iteration 2, the antenna resonated at 4.2 GHz with a fractional bandwidth of 14.3 % (3.9–4.5 GHz). The antenna was further modified in iteration 3 by cutting a rectangular portion from the lower side of the patch. In iteration 3, the antenna resonated at 2.8 GHz, covering a 10-dB bandwidth from 2.5 to 3 GHz (fractional bandwidth of 18.18 %). A couple of changes were made to the antenna in iteration 4. A two slots of length 6.4 mm were etched from the lower-right side of the patch. The ground plane was extended by connecting a hook-shaped stub resonator with it. The two slots and hook-shaped stub resonator combinedly assessed in miniaturization and

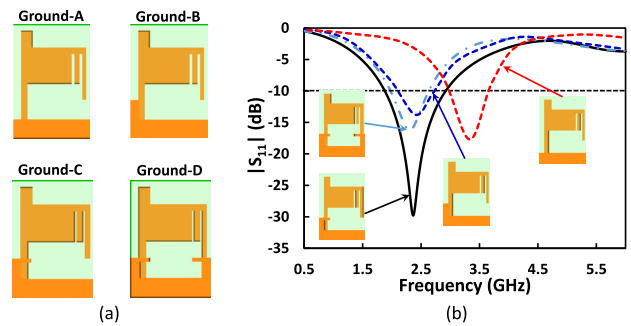


FIGURE 4. (a) Evolution of ground plane, and (b) corresponding reflection coefficient ($|S_{11}|$).

impedance matching. Also, 10-dB bandwidth of the antenna was increased by introducing the hook-shaped stub resonator in the ground plane. In iteration 4 (proposed antenna), the antenna operated at 2.4 GHz with a 10-dB bandwidth from 1.62 GHz to 3 GHz and a fractional bandwidth of 59.7 %, as shown in Fig. 3b.

B. EFFECTS OF GROUND PLANE

The resonance of monopole antenna is based on the size and position of the radiating element and the ground plane. The ground plane of the antenna was optimized using full-wave electromagnetic simulator (HFSS 13.0) for better impedance matching at 2.4 GHz and a wide impedance bandwidth. The impact of different ground plane structure (Fig. 4a) on $|S_{11}|$ of the antenna is portrayed in Fig. 4b. The objective of the ground plane iteration was to achieve a wider bandwidth with better impedance matching at 2.4 GHz. The antenna resonated at 3.4 GHz covering a 10-dB bandwidth from 3 GHz to 3.7 GHz with a fractional bandwidth of 20.8 % for a conventional partial ground plane (Ground-A). The resonant frequency of the antenna shifted to lower frequency side (centered at 2.5 GHz with a fractional bandwidth of 20.4 %) by introducing I-shaped open-circuited stub resonator with ground plane (Ground-B). A frequency shift of around 1 GHz was achieved due to the reactive effect offered by the I-shaped stub resonator. The ground structure was further modified by adding another stub to the I-shaped stub resonator, making it like the hook-shaped (Ground-C). The antenna impedance matching and 10-dB bandwidth was increased by attaching a hook-shaped stub resonator with the ground plane. The antenna in this case operated at 2.4 GHz with a fractional bandwidth of 59.7 %. In type Ground-D antenna, the ground plane was loaded with hook-shaped stub resonator from both ends. In this case, a negligible change in the resonant frequency was seen, however, the fractional bandwidth was reduced to 26.08 %. It is cleared from the study of different ground planes that the hook-shaped stub resonator has a vital role in the impedance matching and miniaturization of the antenna. Ground-C is chosen based on its wide impedance bandwidth and good impedance matching at resonant frequency.

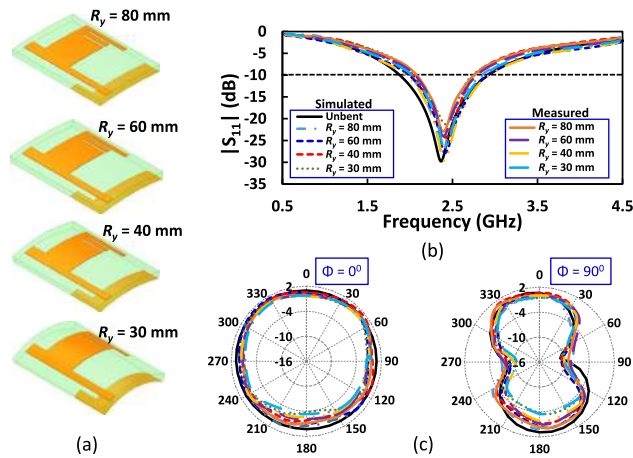


FIGURE 5. (a) Structurally deform antenna bent in y-axis direction (R_y), (b) corresponding simulated and measured reflection coefficient ($|S_{11}|$), and (c) corresponding simulated and measured radiation patterns at 2.4 GHz.

III. ANTENNA ANALYSIS FOR WEARABLE APPLICATIONS

In this section, suitability of the antenna is discussed in on-body worn scenarios. The performance of the antenna in different bending conditions and the electromagnetic exposure on the wearer is thoroughly studied.

A. BENDING ANALYSIS

The antenna in on-body worn scenarios is expected to bend while it is in use. In this section, we studied how the antenna performance varied by bending the antenna in the x-, and y-direction in free space. Different bending radii ($R_y = 80$ mm, 60 mm, 40 mm, 30 mm, $R_x = 80$ mm, 60 mm, 40 mm, 30 mm) were chosen in the x-, and y-direction to study the antenna's $|S_{11}|$, radiation pattern, gain, and efficiency. Fig. 5a portrays structure of the antenna in different bending conditions in the y-axis. The antenna's $|S_{11}|$ and radiation pattern for different bending scenarios in the y-axis is shown in Fig. 5b and Fig. 5c, respectively. It can be well noted that there is a negligible shift in the resonant frequency for all bending scenarios. Also, there is no distortion in the radiation pattern of the antenna in both principal planes at 2.4 GHz. Furthermore, there is a slight reduction in the gain and efficiency of the antenna operated in bending scenarios. Fig. 6a portrays structure of the antenna in different bending conditions in the x-axis. The antenna's $|S_{11}|$ and radiation pattern for different bending scenarios in the x-axis is shown in Fig. 6b and Fig. 6c, respectively. It is obvious that there is a negligible shift in the resonant frequency for all bending scenarios. Also, there is no distortion in the radiation pattern of the antenna in both principal planes at 2.4 GHz. Furthermore, there is a slight reduction in the gain and efficiency of the antenna operated in a bending scenarios. In both cases, the antenna is well matched at the targeted ISM (2.4 GHz) band, though there is a slight change in the resonant frequency. The study shows that the proposed antenna can be used in potential applications where there is a possibility for

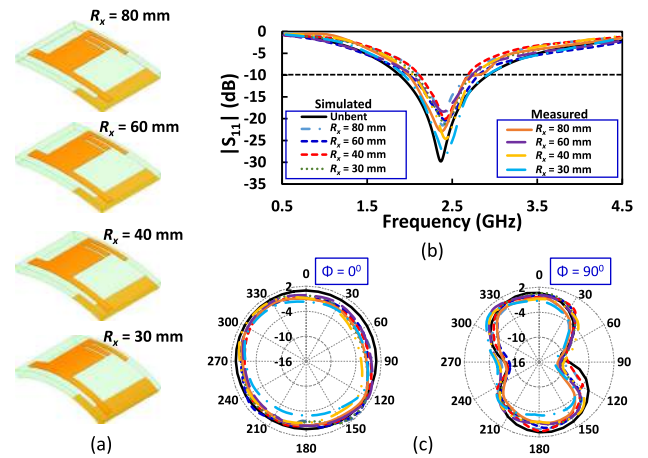


FIGURE 6. (a) Structurally deform antenna bent in x-axis direction (R_x), (b) corresponding simulated and measured reflection coefficient ($|S_{11}|$), and (c) corresponding simulated and measured radiation patterns at 2.4 GHz.

TABLE 1. Comparison of the antenna properties bending in x-axis and y-axis.

Bending in y-axis					
R_y (mm)	Unbent	80	60	40	30
Gain (dBi)	2.50	2.31	2.30	2.35	2.29
Efficiency	93 %	91.1 %	91 %	91.5 %	90.5 %
Bending in x-axis					
R_x (mm)	Unbent	80	60	40	30
Gain (dBi)	2.50	2.45	2.43	2.43	2.41
Efficiency	93 %	92.3 %	92 %	92.2 %	91.7 %

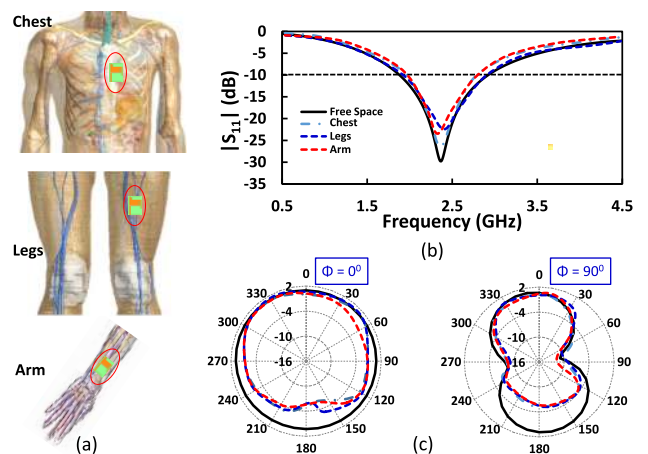


FIGURE 7. (a) Antenna placed on chest, legs and arm, (b) corresponding simulated reflection coefficient ($|S_{11}|$), and (c) corresponding radiation patterns at 2.4 GHz.

the antenna to bend. The overall comparison of the antenna operated in unbent and bent scenarios is given in Table. 1.

B. HUMAN BODY LOADING

The impact of human body loading on performance of the antenna is studied in this section. The antenna was loaded

TABLE 2. Comparison of the antenna properties in the free space and on-body worn scenarios.

Parameter	Free Space	On-body		
		Chest	Legs	Arm
Resonant Frequency (GHz)	2.4	2.3	2.46	2.34
Bandwidth (%)	59.7	34.87	51.6	33.3
VSWR	1.06	1.09	1.17	1.14
Gain (dBi)	2.50	2.2	2.15	2.18
Efficiency (%)	93	80.2	81	81.4
SAR _{1g} (W/kg)	–	6.02	5.99	5.95

on different parts (chest, leg, and arm) of the realistic human model (Fig. 7a) and its performance was analyzed. Fig. 7b shows the simulated $|S_{11}|$, when the antenna was placed on the chest, legs, and arm. The resonant frequency of the loaded antenna was noted at a lower frequency than the free space antenna due to high-permittivity of the human body. The resonant frequency of the antenna was noted at 2.3 GHz with a fractional bandwidth of 34.87 % when placed on the chest. When the antenna was simulated on legs, the resonant frequency shifted to 2.46 GHz with a fractional bandwidth of 51.6 %. The resonant frequency of the antenna was noted at 2.34 GHz with a fractional bandwidth of 33.3 % when placed on the arm. We noted that the fractional bandwidth of the body loaded antenna was lower than the free space antenna, but still the antenna covered the targeted ISM band (2.4 GHz). A negligible impact of the human body loading was seen on the radiation pattern of the antenna, as shown in Fig. 7c. The gain and efficiency of the antenna were reduced in on-body worn scenarios due to lossy nature of the human tissues, muscles, and bones, etc. The effect of electromagnetic exposure on the human body was investigated in terms of a specific absorption rate (SAR) at resonant frequency (2.4 GHz). The SAR of antenna was analyzed on the chest, legs, and arm of the human body. A gap of 6 mm was kept between the human body and antenna for simulating an SAR. An SAR value of 6.02 W/kg, 5.99 W/kg and 5.95 W/kg, averaged over a 1-g tissue was observed for chest, legs, and arm respectively, for the input power of 1 W. However, there are certain limitation on the input power of the devices operating nearby human body [39], [40]. The proposed antenna is safe for use in wearable devices if the input power is less than 265 mW. A photograph of SAR simulation on the chest, arm and leg is reported inside Fig. 8. The detailed summary of the antenna in free-space and on-body worn scenarios is given Table. 2.

IV. EXPERIMENTAL RESULTS

The proposed wearable antenna was fabricated on semi-flexible material of RT/duroid 5880 ($\epsilon_r = 2.2$, $\tan\delta = 0.0004$) using the milling machine. The reflection coefficient of the antenna in free space and on-body worn scenario was measured using a vector network analyzer and the radiation pattern in free space was measured in an anechoic chamber.

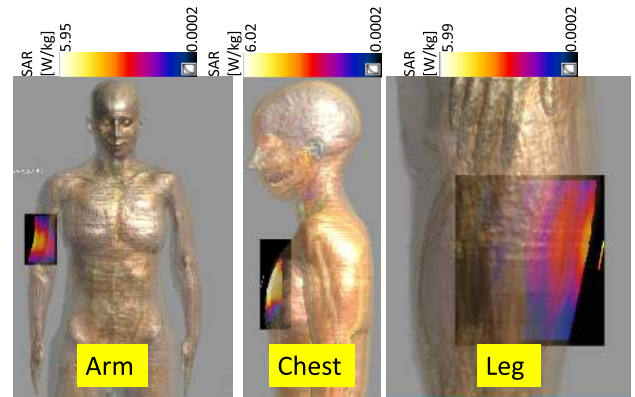


FIGURE 8. Specific absorption rate (SAR_{1g}) of the antenna at 2.4 GHz.

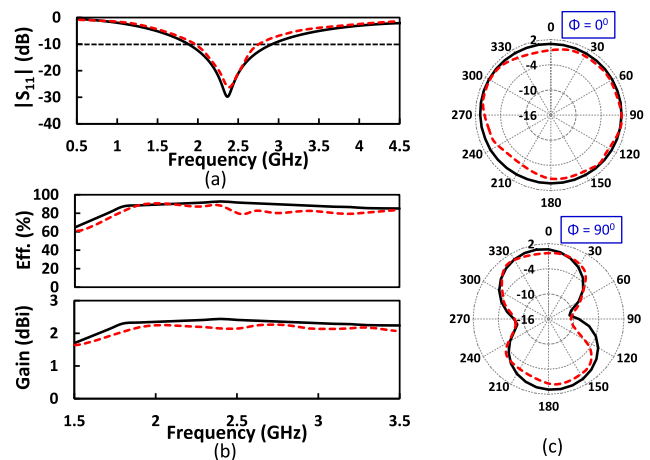


FIGURE 9. Simulated (solid black line) and measured (dashed red line) (a) reflection coefficient ($|S_{11}|$), (b) gain and efficiency, and (c) radiation pattern at 2.4 GHz.

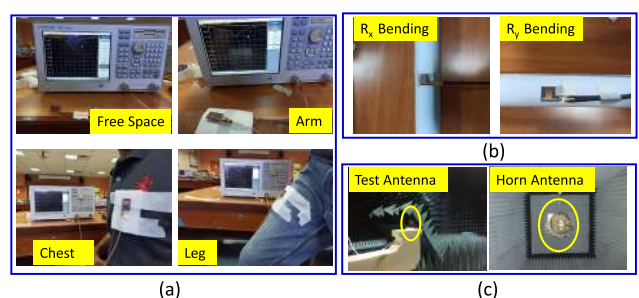


FIGURE 10. (a) Reflection coefficient measurement setup of the antenna for free space, on arm, on chest, and on leg, (b) bending states of the fabricated antenna, and (c) radiation pattern setup.

The measured reflection coefficient, gain, efficiency and radiation pattern of the antenna in free space is illustrated in Fig. 9. The on-body reflection coefficient measurement of the antenna was performed on a 25 years old subject having weight (height) of 70 kg (172.72 cm). The antenna prototype shown in Fig. 10a was placed on different body positions (chest, legs, and arm) for S_{11} measurement. A Styrofoam was

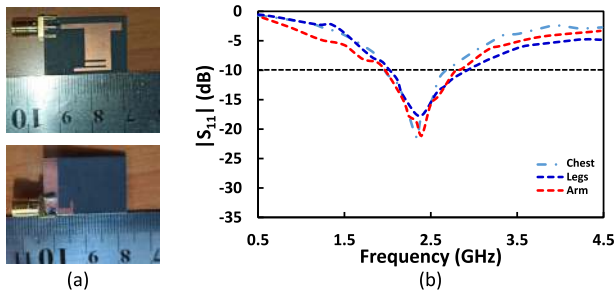


FIGURE 11. (a) Fabricated prototype of the antenna, and (b) measured reflection coefficient of the antenna on different parts of the body.

TABLE 3. Performance comparison with other wearable antennas.

Ref.	Size (λ_g^3)	Frequency Range (GHz)	Bandwidth (%)	Efficiency (%)
[1]	0.63×0.63 ×0.025	~2.3–2.5	8.3	NA
[8]	0.72×0.72 ×0.035	2.28–2.64	14.7	>70
[9]	1.70×1.13 ×0.06	4.30–5.90	34	NA
[13]	0.46×0.46 ×0.006	2.36–2.55	7.75	75
[14]	0.065×0.065 ×0.018	~2.36–2.47	4.5	NA
[15]	0.278×0.316 ×0.018	5.57–5.89	5.5	48
[16]	1.12×1.12 ×0.04	2.40–2.50	4	NA
[17]	1.56×1.56 ×0.04	2.38–2.50	5.08	NA
[18]	0.51×0.40 ×0.019	2.43–2.45 5.72–5.83	1.2 1.9	91 96
[19]	0.62×0.52 ×0.03	2.39–2.51 5.72–5.87	4.9 5.1	72.8 85.6
[20]	0.58×0.58 ×0.03	2.39–2.51	4.9	81
This Work	0.2×0.29 ×0.009	1.62–3	59.7	93

where λ_g is the guided wave length at 2.4 GHz.

used between the body and antenna while the antenna was fixed on the body using sticky tape.

Fig. 9a shows the simulated and measured reflection coefficient of the antenna in free space. The simulated and measured results were matched at the operating band. The simulated (measured) 10-dB bandwidth is 1380 MHz

(980 MHz) and fractional bandwidth is 59.7 % (42.9 %). The simulated gain and efficiency of the antenna was measured and compared with the simulated results as shown in Fig. 9b. We see that there is a negligible mismatch in the simulated and measured results in terms of gain and efficiency. The radiation pattern of the antenna in both principal planes ($\phi = 0^\circ$ and $\phi = 90^\circ$) was measured in echo-free anechoic chamber and is compared with the simulated results in Fig. 9c. Fig. 11b shows the measured reflection coefficient of the antenna when it was worn on the chest, legs, and arm. We see that the resonant frequency of the antenna in all wearing cases (on the chest, leg, and arm) is 2.4 GHz. The 10-dB on-body measured bandwidths of 708 MHz (on chest), 912 MHz (on leg), and 856 MHz (on arm) with fractional bandwidths of 31.4 % (on chest), 37.2 % (on leg), and 36.1 % (on arm) were noted when the antenna was placed on the chest, leg and arm of the human body. The mismatch between the on-body simulated and measured values is because of the SMA losses, cable losses and imperfection in the calibration of the measurement devices.

A comparison table (Table. 3) is presented to portray advantages of the proposed antenna over the existing wearable antennas at ISM band. The proposed antenna is compared with similar work present in the literature in terms of size, bandwidth and efficiency. We see that our proposed antenna has a low profile than other antennas. Also, the fractional bandwidth of our antenna is more than the other antennas, which in turn make the antenna suitable for wearable applications.

V. CONCLUSION

We have designed a low-profile, wideband antenna for wearable biomedical devices. The miniaturization of the antenna has been realized by introduction of rectangular slots in the conventional rectangular patch and the bandwidth has been enhanced using a hook-shaped stub resonator with the ground plane. The designed antenna resonated 2.4 GHz with a 10-dB bandwidth (fractional bandwidth) of 1380 MHz (59.7 % at the centre frequency of 2.4 GHz). The proposed antenna maintained high gain and efficiency in the free space and in the body worn case. Moreover, the antenna shows reasonable performance when it is bent along the x-axis and y-axis. Also, SAR_{1g} value of the antenna is in the limits (< 1.6 W/kg for an input power of less than 265 mW) specified by the IEEE. The proposed wideband antenna is a promising candidate for compact wearable biomedical devices because of its low size, wideband and better performance on human body loading case. The high data rate transmission ability of the antenna can be further enhanced by designing a circularly polarized antenna with multiple-input multiple-output (MIMO) architecture.

REFERENCES

[1] A. Y. I. Ashyap, Z. Zainal Abidin, S. H. Dahlan, H. A. Majid, M. R. Kamarudin, A. Alomainy, R. A. Abd-Alhameed, J. S. Kosha, and J. M. Noras, "Highly efficient wearable CPW antenna enabled by EBG-FSS structure for medical body area network applications," *IEEE Access*, vol. 6, pp. 77529–77541, 2018.

- [2] M. Suzan Miah, A. N. Khan, C. Icheln, K. Haneda, and K.-I. Takizawa, "Antenna system design for improved wireless capsule endoscope links at 433 MHz," *IEEE Trans. Antennas Propag.*, vol. 67, no. 4, pp. 2687–2699, Apr. 2019.
- [3] A. Basir and H. Yoo, "A stable impedance-matched ultrawideband antenna system mitigating detuning effects for multiple biotelemetric applications," *IEEE Trans. Antennas Propag.*, vol. 67, no. 5, pp. 3416–3421, May 2019.
- [4] A. Sharma, E. Kampianakis, and M. S. Reynolds, "A dual-band HF and UHF antenna system for implanted neural recording and stimulation devices," *IEEE Antennas Wireless Propag. Lett.*, vol. 16, pp. 493–496, 2017.
- [5] L. W. Liu, A. Kandwal, Q. Cheng, H. Shi, I. Tobore, and Z. Nie, "Non-invasive blood glucose monitoring using a curved Goubau line," *Electronics*, vol. 8, no. 6, p. 662, Jun. 2019.
- [6] S. A. A. Shah and H. Yoo, "Scalp-implantable antenna systems for intracranial pressure monitoring," *IEEE Trans. Antennas Propag.*, vol. 66, no. 4, pp. 2170–2173, Apr. 2018.
- [7] M. W. A. Khan, A. Khan, M. Rizwan, L. Sydanheimo, T. Bjorninen, L. Ukkonen, and Y. Rahmat-Samii, "Loop antenna for deep implant powering in an intracranial pressure monitoring system," in *Proc. IEEE Int. Symp. Antennas Propag. USNC/URSI Nat. Radio Sci. Meeting*, Jul. 2018, pp. 207–208.
- [8] G.-P. Gao, B. Hu, S.-F. Wang, and C. Yang, "Wearable circular ring slot antenna with EBG structure for wireless body area network," *IEEE Antennas Wireless Propag. Lett.*, vol. 17, no. 3, pp. 434–437, Mar. 2018.
- [9] A. Alemaryeen and S. Noghianian, "On-body low-profile textile antenna with artificial magnetic conductor," *IEEE Trans. Antennas Propag.*, vol. 67, no. 6, pp. 3649–3656, Jun. 2019.
- [10] A. Basir, A. Bouazizi, M. Zada, A. Iqbal, S. Ullah, and U. Naem, "A dual-band implantable antenna with wide-band characteristics at MICS and ISM bands," *Microw Opt Technol Lett*, vol. 60, no. 12, pp. 2944–2949, Dec. 2018.
- [11] A. Bouazizi, G. Zaibi, A. Iqbal, A. Basir, M. Samet, and A. Kachouri, "A dual-band case-printed planar inverted-F antenna design with independent resonance control for wearable short range telemetric systems," *Int. J. RF Microw. Comput.-Aided Eng.*, vol. 29, no. 8, p. e21781, 2019.
- [12] A. Michel, R. Colella, G. A. Casula, P. Nepa, L. Catarinucci, G. Montisci, G. Mazzarella, and G. Manara, "Design considerations on the placement of a wearable UHF-RFID PIFA on a compact ground plane," *IEEE Trans. Antennas Propag.*, vol. 66, no. 6, pp. 3142–3147, Jun. 2018.
- [13] A. Arif, M. Zubair, M. Ali, M. U. Khan, and M. Q. Mehmood, "A compact, low-profile fractal antenna for wearable on-body WBAN applications," *IEEE Antennas Wireless Propag. Lett.*, vol. 18, no. 5, pp. 981–985, May 2019.
- [14] C. Mohan and S. E. Florence, "Miniaturised triangular microstrip antenna with metamaterial for wireless sensor node applications," *IETE J. Res.*, pp. 1–6, Jul. 2019.
- [15] Y. J. Li, Z. Y. Lu, and L. S. Yang, "CPW-fed slot antenna for medical wearable applications," *IEEE Access*, vol. 7, pp. 42107–42112, 2019.
- [16] S. Zhu and R. Langley, "Dual-band wearable textile antenna on an EBG substrate," *IEEE Trans. Antennas Propag.*, vol. 57, no. 4, pp. 926–935, Apr. 2009.
- [17] S. Velan, E. F. Sundarsingh, M. Kanagasabai, A. K. Sarma, C. Raviteja, R. Sivasamy, and J. K. Pakkathillam, "Dual-band EBG integrated monopole antenna deploying fractal geometry for wearable applications," *IEEE Antennas Wireless Propag. Lett.*, vol. 14, pp. 249–252, 2015.
- [18] X.-Q. Zhu, Y.-X. Guo, and W. Wu, "A compact dual-band antenna for wireless body-area network applications," *IEEE Antennas Wireless Propag. Lett.*, vol. 15, pp. 98–101, 2016.
- [19] S. Agneessens and H. Rogier, "Compact half diamond dual-band textile HMSIW on-body antenna," *IEEE Trans. Antennas Propag.*, vol. 62, no. 5, pp. 2374–2381, May 2014.
- [20] S. Agneessens, S. Lemey, T. Vervust, and H. Rogier, "Wearable, small, and robust: The circular quarter-mode textile antenna," *IEEE Antennas Wireless Propag. Lett.*, vol. 14, pp. 1482–1485, 2015.
- [21] P. Salonen and L. Hurme, "A novel fabric WLAN antenna for wearable applications," in *Proc. IEEE Antennas Propag. Soc. Int. Symp. Dig. Held Conjoint., USNC/CNC/URSI North Amer. Radio Sci. Meeting*, Mar. 2004.
- [22] M. Klemm, I. Locher, and G. Troster, "A novel circularly polarized textile antenna for wearable applications," in *Proc. 7th Eur. Conf. Wireless Technol.*, 2004, pp. 285–288.
- [23] B. Sanz-Izquierdo, F. Huang, and J. Batchelor, "Small size wearable button antenna," in *Proc. 1st Eur. Conf. Antennas Propag.*, Nov. 2006, pp. 1–4.
- [24] Y.-H. Kim and Y.-C. Chung, "UHF RFID dipole tag antenna design using flexible electro-thread," *J. Korean Inst. Electromagn. Eng. Sci.*, vol. 19, no. 1, pp. 1–6, Jan. 2008.
- [25] S. Sankaralingam and B. Gupta, "A circular disk microstrip WLAN antenna for wearable applications," in *Proc. Annu. IEEE India Conf.*, Dec. 2009, pp. 1–4.
- [26] M. M. Mansor, S. K. A. Rahim, and U. Hashim, "A CPW-fed 2.45 GHz wearable antenna using conductive nanomaterials for on-body applications," in *Proc. IEEE REGION 10 Symp.*, Apr. 2014, pp. 240–243.
- [27] H. Wong, K. K. So, K. B. Ng, K. M. Luk, C. H. Chan, and Q. Xue, "Virtually shorted patch antenna for circular polarization," *IEEE Antennas Wireless Propag. Lett.*, vol. 9, pp. 1213–1216, 2010.
- [28] J. Kula, D. Psychoudakis, W.-J. Liao, C.-C. Chen, J. Volakis, and J. Halloran, "Patch-antenna miniaturization using recently available ceramic substrates," *IEEE Antennas Propag. Mag.*, vol. 48, no. 6, pp. 13–20, Dec. 2006.
- [29] C. Liu, Y.-X. Guo, and S. Xiao, "Capacitively loaded circularly polarized implantable patch antenna for ISM band biomedical applications," *IEEE Trans. Antennas Propag.*, vol. 62, no. 5, pp. 2407–2417, May 2014.
- [30] A. Pourghorban Saghati, J. Singh Batra, J. Kameoka, and K. Entesari, "Miniature and reconfigurable CPW folded slot antennas employing liquid-metal capacitive loading," *IEEE Trans. Antennas Propag.*, vol. 63, no. 9, pp. 3798–3807, Sep. 2015.
- [31] J. Wang and O. Fujiwara, "Reduction of electromagnetic absorption in the human head for portable telephones by a ferrite sheet attachment," *IEICE Trans. Commun.*, vol. 80, no. 12, pp. 1810–1815, 1997.
- [32] A. Hirata, T. Adachi, and T. Shiozawa, "Folded-loop antenna with a reflector for mobile handsets at 2.0 GHz," *Microw. Opt. Technol. Lett.*, vol. 40, no. 4, pp. 272–275, Feb. 2004.
- [33] K. Agarwal, Y.-X. Guo, and B. Salam, "Wearable AMC backed near-endfire antenna for on-body communications on latex substrate," *IEEE Trans. Compon., Packag., Manuf. Technol.*, vol. 6, no. 3, pp. 346–358, Mar. 2016.
- [34] Z. H. Jiang, Z. Cui, T. Yue, Y. Zhu, and D. H. Werner, "Compact, highly efficient, and fully flexible circularly polarized antenna enabled by silver nanowires for wireless body-area networks," *IEEE Trans. Biomed. Circuits Syst.*, vol. 11, no. 4, pp. 920–932, Aug. 2017.
- [35] P. Prakash, M. P. Abegaonkar, A. Basu, and S. K. Koul, "Gain enhancement of a CPW-fed monopole antenna using polarization-insensitive AMC structure," *IEEE Antennas Wireless Propag. Lett.*, vol. 12, pp. 1315–1318, 2013.
- [36] A. Iqbal, A. Basir, A. Smida, N. K. Mallat, I. Elfergani, J. Rodriguez, and S. Kim, "Electromagnetic bandgap backed millimeter-wave MIMO antenna for wearable applications," *IEEE Access*, vol. 7, pp. 111135–111144, 2019.
- [37] C. A. Balanis, *Antenna Theory: Analysis and Design*. Hoboken, NJ, USA: Wiley, 1997.
- [38] Z. N. Chen, T. S. P. See, and X. Qing, "Small printed ultrawideband antenna with reduced ground plane effect," *IEEE Trans. Antennas Propag.*, vol. 55, no. 2, pp. 383–388, Feb. 2007.
- [39] A. Iqbal, A. Smida, L. F. Abdulrazak, O. A. Saraereh, N. K. Mallat, I. Elfergani, and S. Kim, "Low-profile frequency reconfigurable antenna for heterogeneous wireless systems," *Electronics*, vol. 8, no. 9, p. 976, Sep. 2019.
- [40] C. Zebiri, D. Sayad, I. Elfergani, A. Iqbal, W. F. Mshwat, J. Kosha, J. Rodriguez, and R. Abd-Alhameed, "A compact semi-circular and arc-shaped slot antenna for heterogeneous RF front-ends," *Electronics*, vol. 8, no. 10, p. 1123, Oct. 2019.



AMOR SMIDA received the degree in electronic baccalaureate and the M.Sc. degree in analyze and digital processing of the electronic systems in 2008 and 2010, respectively, and the Ph.D. degree from Faculty of Mathematical, Physical and Natural Sciences of Tunis, Tunis El-Manar University, Tunisia, in 2014. From 2008 to 2014, he was a Graduate Student Researcher with the Unit of Research in High Frequency Electronic Circuits and Systems. Since August 2014, he has been an Assistant Professor with the Department of Medical Equipment Technology, College of Applied Medical Sciences, Majmaah University, Saudi Arabia. His current researches focus on smart antennas, biosensors, biomedical applications, neural network applications in antennas, adaptive arrays, and microwave circuits design CST studio microwave.



AMJAD IQBAL (Student Member, IEEE) received the degree in electrical engineering from the COMSATS Institute of Information Technology, Islamabad, Pakistan, in 2012, and the M.S degree in electrical engineering from the Department of Electrical Engineering, CECOS University of IT and Emerging Science, Peshawar, Pakistan, in 2018. He is currently pursuing the Ph.D. degree with the Faculty of Engineering, Multimedia University, Cyberjaya, Selangor,

Malaysia. He worked as a Lab Engineer with the Department of Electrical Engineering, CECOS University, Peshawar, from 2016 to 2018. His research interests include printed antennas, flexible antennas, implantable antennas, MIMO antennas, dielectric resonator antennas, and synthesis of microwave components.



ABDULLAH J. ALAZEMI (Member, IEEE) received the B.S. degree in electrical engineering from Kuwait University, in 2010, and the M.S and Ph.D. degrees in electrical and computer engineering from the University of California at San Diego, La Jolla, CA, USA, in 2013 and 2015, respectively. He joined the Department of Electrical Engineering, Kuwait University, where he is currently an Assistant Professor. His work focuses on tunable antennas and filters with RF-MEMS, multiband

power dividers and couplers for advanced communication systems, and MM-wave to THz Quasi-optical systems.



MOHAMED I WALY received the degree in biomedical engineering and system baccalaureate and the M.Sc. degree in biomedical engineering and system in 2004 and 2009, respectively, and the Ph.D. degree from the Faculty of Biomedical Engineering and System, Cairo University, in 2013. From 2004 to 2015, he was a Consultant Engineer with CASBEC, from 2013 to 2015. Since October 2015, he has been an Assistant Professor with the Department of Medical Equipment

Technology, College of Applied Medical Sciences, Majmaah University, Saudi Arabia. His current researches focus on smart antennas, biosensors, biomedical applications, machine learning applications in medical field, mechanics, biomechanics applications, and predication disease model.



RIDHA GHAYOULA received the Dipl. Eng. degree in electrical engineering and the M.Sc. degree in analyze and digital processing of the electronic systems in 2002 and 2005, respectively, and the Ph.D. degree from Faculty of Mathematical, Physical, and Natural Sciences of Tunis, Tunis El-Manar University, Tunisia, in 2008. From 2004 to 2012, he was a Graduate Student Researcher with the Unit of Research in High Frequency Electronic Circuits and Systems. He has

worked on several industrial experiences in Canada as an FPGA Designer with 2014 with Aerostar Research and Development, Doric Lenses, Inc., in 2017, Telops, Inc., in 2018, and M2S Electronics, Canada, in 2019. Since August 2009, he has been an Assistant Professor with the Electrical Engineering Department, Higher Institute of Computer Science of El Manar, Tunisia, and an Associate Professor from 2014 to 2015. Since May 2012, he has been a Postdoctoral Fellow with LRTS, Department of Electrical and Computer Engineering, Laval University, Quebec, QC, Canada. His current researches focus on software engineering, FPGA, softcore processor, modeling and simulation, TDOA, DOA, phased arrays, smart antennas, direction finding, radio-communication systems, neural network applications in antennas, adaptive arrays, and microwave circuits design. He has published more than 75 journals and conference papers on smart antennas and embedded systems.

Dr. Ghayoula participated in several industrial projects in North America for five years in the embedded field, real time, LidAR, and FPGA, for example, Dual optogenetic stimulation with a Laser Diode Fiber Light Source, Hyperspectral IR Cameras, DE-8209 ORKAN—UP15 (C0069A), HVAC Application: TNG15-TX070, HVAC Application: DE-8209 TOUCH18 WiFi-TX120.



SUNGHWAN KIM received the B.S., M.S., and Ph.D. degrees from Seoul National University, South Korea, in 1999, 2001, and 2005, respectively. He was a Postdoctoral Visitor with the Georgia Institute of Technology (GeorgiaTech), from 2005 to 2007 and a Senior Engineer with Samsung Electronics, from 2007 to 2011. He is currently an Associate Professor with the School of Electrical Engineering, University of Ulsan, South Korea.

His main research interests are channel coding, modulation, massive MIMO, visible light communication, and quantum information.

...